

Intense terahertz pulses by four-wave rectification in air

D. J. Cook and R. M. Hochstrasser

Department of Chemistry, University of Pennsylvania, 231 S. 34th Street, Philadelphia, Pennsylvania 19104-6323

Received April 19, 2000

We describe a new four-wave rectification method for the generation of intense, ultrafast terahertz (THz) pulses from gases. The fundamental and second-harmonic output of an amplified Ti:sapphire laser is focused to a peak intensity of $\sim 5 \times 10^{14}$ W/cm². Under these conditions, peak THz fields estimated at 2 kV/cm have been observed; the measured power spectrum peaks near 2 THz. Phase-dependent measurements show that this is a coherent process and is sensitive to the relative phases of the fundamental and second-harmonic pulses. Comparable THz signals have been observed from nitrogen and argon as well as from air. © 2000 Optical Society of America

OCIS codes: 320.7110, 320.7160, 190.4380, 260.3090.

The technology associated with the generation and detection of ultrafast terahertz (THz) pulses has benefited from recent research. Nonetheless, the selection of a method for generating THz pulses involves compromises between peak field and bandwidth. Furthermore, self-absorption in the materials used for the generation of THz radiation leads to spectral gaps in wideband sources. The methods for the generation of THz pulses can be categorized as either rectification sources or transient current sources. Examples of transient current sources are point source antennae and large-aperture biased emitters.¹ Rectification sources rely on the nonvanishing $\chi^{(2)}$ of materials such as ZnTe and GaAs.² Here we report a new method for the generation of ultrafast THz pulses in which optical pulses at ω_0 and $2\omega_0$ focused in gases such as ambient air generate sufficient THz intensity and bandwidth to be useful as practical THz sources. The initial investigations of the nature of this signal are consistent with the hypothesis that the THz radiation is generated by a new coherent nonlinear process, which appears related to four-wave rectification (FWR).

In a FWR process, the carrier frequencies of three input fields add to zero, and the nonlinear response is driven by the product of the field envelopes of the input pulses. In one possible mechanism for FWR, the nonlinear polarization induced by the input waves acts as the source of the THz radiation. This process is essentially the inverse of the previously reported THz field-induced second-harmonic generation method, in which the THz field and an optical field at ω_0 interact to generate an optical field at $2\omega_0$.³ A weak signal from air was observed in our initial THz field-induced second-harmonic generation experiments but was not included in our initial report, which emphasized liquid-phase dynamics.

A regeneratively amplified Ti:sapphire laser system provided ~ 65 -fs, 800-nm pulses at a repetition rate of 1 kHz. For the FWR method, 150 μ J of energy was focused through a 100- μ m-thick β -barium borate (BBO) crystal phased matched for second-harmonic generation and then to a beam waist where the THz radiation is generated. The peak optical intensity at the focus is estimated to be 5×10^{14} W/cm². A 50-mm clear

aperture, $f/1.5$ off-axis paraboloid collimates the THz radiation and a 44.5-mm clear aperture, $f/0.86$ off-axis paraboloid focuses it onto the 250- μ m-thick ZnTe crystal used for electro-optical (EO) detection. The majority of the optical energy used to generate the THz radiation passes through a hole in the paraboloid that was used to collect the THz radiation, and a subsequent Si window is used to filter the residual scattered light. For most of the experiments reported here, the THz radiation was generated in ambient air. Experiments in which the beam waist was purged through a slit orifice with either nitrogen or argon were also conducted.

We completed a number of tests to determine whether the signal depends on both 400- and 800-nm radiation. A Si window placed between the BBO crystal and the focus eliminated the THz signal, ruling out a rectification process in the BBO crystal. If the BBO crystal was removed, a THz signal persisted when only 800-nm light was present. However, the intensity in the absence of the 400-nm light was a factor of 4000 smaller than the FWR intensity. When a 4.75-mm-thick fused-silica window was placed between the BBO crystal and the focus, the difference between the 400- and 800-nm group velocities delayed the 400-nm pulse by 750 fs relative to the 800-nm pulse, leading to a loss of overlap between the pulses. Under these conditions the signal was greatly reduced and resembled that which was obtained in the absence of the BBO crystal.

Power- and polarization-dependent measurements were conducted. The power of the 800-nm input (before the BBO crystal) was varied with a half-wave plate and a polarizer. The polarization-sensitive measurements utilized the inherent polarization sensitivity of the EO detection method. Orthogonal polarization components can be measured by 90° rotation of the ZnTe crystal. However, the EO signal must be optimized following rotation of the crystal; this leads to a significant (approximately 10–20%) uncertainty in the magnitude of these measurements. The alignment of the EO crystal and the efficacy of the EO method as a probe of polarization were confirmed with a wire grid polarizer.

Finally, we determined the dependence on the relative phases of the 400- and 800-nm pulses by inserting

a 150- μm -thick quartz microscope coverslip between the BBO crystal and the focus and varying the angle of incidence.

The time-dependent electrical field of the THz pulse generated in flowing nitrogen gas is displayed in Fig. 1(a), and the Fourier-transformed power spectrum is depicted in Fig. 1(b). The EO detection measures the retardance of an optical probe pulse induced by the electric field of the THz pulse. The observed retardance is the convolution of the time-dependent electric field of the THz pulse and the linear response of the probe and THz pulses as they travel through the Pockels material.⁴ If the effects of the linear response of the ZnTe Pockels crystal (i.e., group-velocity mismatch, dispersion, and absorption) are negligible over the length of the crystal, the time-dependent THz field is proportional to the retardance.⁵ If the area A of the THz beam waist in the EO crystal is known, the energy of the THz pulse, $W \approx \epsilon_0 c n A \int_{-\infty}^{\infty} E^2(t) dt$, can then be estimated. THz fluences in the ZnTe crystal as large as 10 nJ cm⁻² have been measured. The assumption of a diffraction-limited THz beam waist ($\approx 250 \mu\text{m}$) yields a detected energy of ~ 5 pJ.

A THz signal generated by a polarization-driven FWR process will depend on the relative phase of the fundamental and second-harmonic pulses. For the gases studied here, the third-order susceptibility that might arise from the neutral or field-ionized sample will be considered to be instantaneous, leading to a third-order polarization:

$$P_i^{(3)}(t) = \gamma_{ijkl} E_j^{2\omega_0}(t) E_k^{\omega_0}(t) E_l^{\omega_0}(t). \quad (1)$$

Associating E_k and E_l with the 800-nm pulse (ω_0) leads to $E_k(t) = E_l(t) = 1/2 E_{800}(t) \exp(i\omega_0 t) + \text{c.c.}$ Likewise, $E_j = 1/2 E_{400}(t) \exp[i(2\omega_0 t + \varphi)] + \text{c.c.}$, where φ is the phase difference between the two pulses. The product of the fields results in a $4\omega_0$ term, a $2\omega_0$ term, and a rectified term. Noting that the 400-nm radiation is generated by second-harmonic generation from the 800-nm pulse, we find that $E_{400}(t) \propto E_{800}^2(t)$ and

$$P_i^{(3)}(t) \propto E_{800}^4(t) \cos \varphi. \quad (2)$$

Because the size of the focal region is of the order of the wavelength of the emitted THz radiation, the point source solution to Maxwell's equations dictates that, in the far field, $E_{\text{THz}}(t) \propto \ddot{P}(t)$. The initial waveform appears to be the second derivative of the product of optical pulse envelopes; this is followed by etalon reflections from the ZnTe EO crystal and the Si filter and by a free induction decay associated with resonances in ZnTe and atmospheric water. The dashed curve in Fig. 1(b) represents the anticipated spectrum from the second derivative of relation (2), assuming a 120-fs Gaussian intensity envelope and an ideal detector.

The necessary phase locking of the fundamental and second-harmonic pulses is achieved by use of the output from the BBO crystal, with no intervening optics, to generate the THz radiation. In the phase-dependence experiment, a microscope coverslip is placed between the BBO and the focus. The phase

difference is determined by the angle of incidence. The results of the phase-dependence measurement, which are depicted in Fig. 2, are consistent with a FWR model.

We examined the effects of various gas compositions by purging the focal region with nitrogen and argon gases. In terms of THz pulse energy, the ratio of the signals obtained from argon and nitrogen is 2.2. If the FWR process were driven by the electric-field-induced second harmonic $\chi^{(3)}$ of the gases,⁶ we would expect an argon/nitrogen ratio of 1.6. We have no estimate of the ratio for a field-ionization-driven process.

The results of the power-dependent measurements are shown in Fig. 3. Because of the aforementioned phase considerations, the 800- and 400-nm powers were not adjusted separately. Rather, the 800- and 400-nm intensities after the BBO crystal were measured as a function of 800-nm input intensity before the lens and the BBO crystal. The THz intensity was fitted to $I_{400} I_{800}^p$, which yielded a value of 3.1 ± 0.4 for p . That this measurement yields a value greater than the anticipated value of 2 indicates that other consecutive processes, such as ionization and the formation of excited states (see below), could lead to the enhanced hyperpolarizability.

The vertical-to-horizontal polarization ratio for the generated THz was measured with a vertically

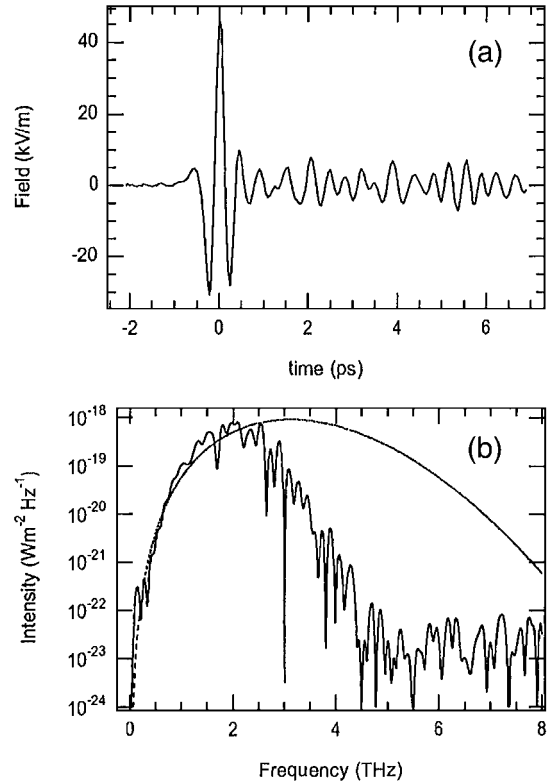


Fig. 1. (a) Time-dependent THz field from FWR in nitrogen gas, (b) the associated power spectrum. The linear response of the ZnTe detector is neglected in the estimation of the field and the calculation of the spectrum. The spectrum at frequencies above 3 THz is perturbed by the 5.3-THz transverse optical phonon resonance in the ZnTe crystal used for the EO detection. Dashed curve, the spectrum anticipated from a rectified 240-fs pulse, assuming ideal detection.

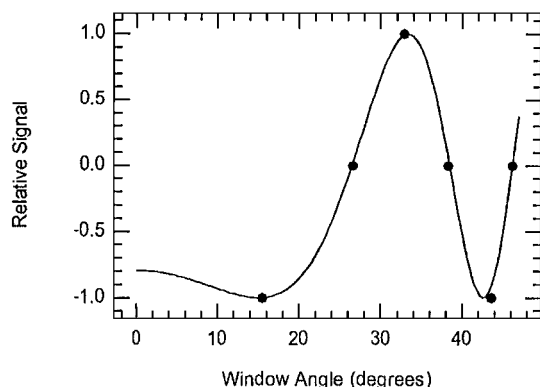


Fig. 2. Results of the phase-dependent experiments. The angle of incidence on a microscope coverslip between the BBO and the focus was tuned, and the angles associated with maxima (relative signal 1), minima (relative signal -1), and zero crossings (relative signal 0) were recorded. Solid curve, a least-squares fit to the data.

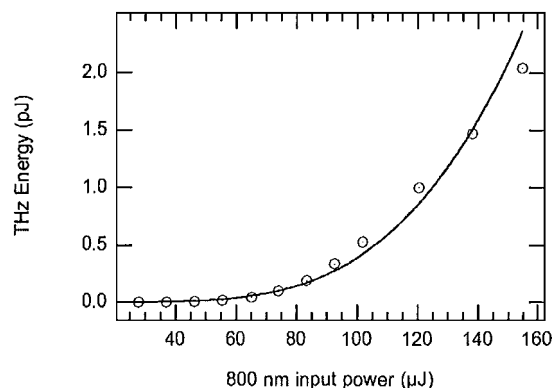


Fig. 3. Results of the power-dependent measurements. Solid curve, a least-squares fit to the data. A type II BBO crystal was used to generate the 400-nm pulses for this experiment. A type I crystal was used for the other measurements presented here.

polarized fundamental pulse and a horizontally polarized second-harmonic pulse, and a ratio of 0.04 was obtained. For a process that depends on third-order polarization in an isotropic nonresonant medium, the only nonvanishing susceptibility tensors are χ_{iiii} and χ_{ijij} . A $P^{(3)}$ FWR model therefore predicts that the generated THz radiation will have the same polarization as the $2\omega_0$ input; although this is essentially what was observed it does not prove the FWR mechanism.

THz radiation has also been observed from wake fields associated with high-intensity (10^{18} – 10^{19} -W/cm²) laser-induced plasmas.⁷ Furthermore, the GaAs-based coherently controlled photocurrent THz source reported by Côté *et al.* uses ω_0 and $2\omega_0$ input pulses and exhibits phase-sensitive behavior.⁸ The maximum intensity of the optical pulses used for the results reported here ($\sim 5 \times 10^{14}$ W/cm²) corresponds to a field of 0.4 V/nm. At this intensity,

field ionization of nitrogen and oxygen might become significant.⁹ Although the ionization rate is a strongly varying function of laser intensity, it is not necessarily discernable in the power-dependent measurements, which were limited to half a decade of power. It is also possible that the generation of excited states and Rydberg species could lead to an enhanced hyperpolarizability. The weak THz signal that persists in the absence of the 400-nm pulse has not yet been fully explained. A rectified signal from a single input frequency necessitates either an even-order process associated with a density gradient in ionized or excited species or a parametric third-order process.

The intensity of the THz radiation generated by the FWR process in ambient air is surprisingly strong. Without further optimization, it already constitutes a practical source for THz experiments, with fields of the same order of magnitude as $\chi^{(2)}$ rectification sources. Rectification of shorter pulses in these nonpolar gases with no far-IR absorption could lead to enhanced bandwidth, with no spectral limitations associated with self-absorption in the medium used to generate the THz radiation. Furthermore, if three different frequencies, one (ω') near $2\omega_0$ and two (ω'' and ω''') near ω_0 , are used for the input pulses, frequency generation at $\omega' - \omega'' - \omega'''$ in the hitherto problematic region between 100 and 1000 cm⁻¹ should be, in principle, possible. Finally, variation of the gas pressures could expose threshold behavior and allow optimization of the intensity. Further experiments are necessary if the mechanism for the generation of this radiation is to be fully understood.

This study was supported by the National Institutes of Health and the National Science Foundation and by Research Resource grant RR13456. R. M. Hochstrasser's e-mail address is hochstra@sas.upenn.edu.

References

1. J. T. Darrow, B. B. Hu, X.-C. Zhang, and D. H. Auston, *Opt. Lett.* **15**, 323 (1990); C. Fattinger and D. Grischkowsky, *Appl. Phys. Lett.* **53**, 1480 (1988).
2. X.-C. Zhang, Y. Jin, and X. F. Ma, *Appl. Phys. Lett.* **61**, 2764 (1992); T. Yajima and N. Takeuchi, *Jpn. J. Appl. Phys.* **9**, 1361 (1970).
3. D. J. Cook, J. X. Chen, E. A. Morlino, and R. M. Hochstrasser, *Chem. Phys. Lett.* **309**, 221 (1991).
4. H. J. Bakker, G. C. Cho, H. Kurz, Q. Wu, and X.-C. Zhang, *J. Opt. Soc. Am. B* **15**, 1795 (1998).
5. C. Winnewisser, P. U. Jepsen, M. Schall, V. Schyja, and H. Helm, *Appl. Phys. Lett.* **70**, 3069 (1997).
6. D. P. Shelton, *Phys. Rev. A* **42**, 2578 (1990).
7. H. Hamster, A. Sullivan, S. Gordon, W. White, and R. W. Falcone, *Phys. Rev. Lett.* **71**, 2725 (1993).
8. D. Côté, J. M. Fraser, M. DeCamp, P. H. Bucksbaum, and H. M. van Driel, *Appl. Phys. Lett.* **75**, 3959 (1999).
9. A. Talebpour, J. Yang, and S. L. Chin, *Opt. Commun.* **163**, 29 (1999).